ARTICLE

Rotationally Resolved Vacuum Ultraviolet Pulsed Field Ionization-Photoelectron Vibrational Bands for $H_2^+(X^2\Sigma_g^+, v^+=0\text{-}18)$†

Chao Chang[a], Cheuk-Yiu Ng[a]*, S. Stimson[b], M. Evans[b], C. W. Hsu[b]

a. Department of Chemistry, University of California, Davis, Davis, CA 95616, USA;
b. Ames Laboratory, USDOE and Department of Chemistry, Iowa State University, Ames, IA 50011, USA

(Dated: Received on May 16, 2007; Accepted on June 2, 2007)

We have obtained a rotationally resolved vacuum ultraviolet pulsed field ionization-photoelectron (VUV-PFI-PE) spectrum of H_2 in the energy range of 15.30-18.09 eV, covering the ionization transitions $H_2^+(X^2\Sigma_g^+, v^+=0\text{-}18, N^+=0\text{-}5) \leftarrow H_2(X^1\Sigma_g^+, v''=0, J''=0\text{-}4)$. The assignment of the rotational transitions resolved in the VUV-PFI-PE vibrational bands for $H_2^+(X^2\Sigma_g^+, v^+=0\text{-}18)$ and their simulation using the Buckingham-Orr-Sichel (BOS) model are presented. Only the $\Delta N=N^+-J''=0$ and ±2 rotational branches are observed in the VUV-PFI-PE spectrum of H_2. However, the vibrational band is increasingly dominated by the $\triangle N=0$ rotational branch as v^+ is increased. The BOS simulation reveals that the perturbation of VUV-PFI-PE rotational line intensities by near-resonance autoionizing Rydberg states is minor at $v^+\geq6$ and decreases as v^+ is increased. Thus, the rotationally resolved PFI-PE bands for $H_2^+(v^+\geq6)$ presented here provide reliable estimates of state-to-state cross sections for direct photoionization of H_2, while the rotationally resolved PFI-PE bands for $H_2^+(v^+\leq5)$ are useful data for fundamental understanding of the near resonance autoionizing mechanism. On the basis of the rovibrational assignment of the VUV-PFI-PE spectrum of H_2, the ionization energies for the formation of $H_2^+(X^2\Sigma_g^+, v^+=0\text{-}18, N^+=0\text{-}5)$ from $H_2^+(X^1\Sigma_g^+, v''=0, J''=0\text{-}4)$, the vibrational constants (ω_e, $\omega_e\chi_e$, $\omega_e y_e$, and $\omega_e z_e$), the rotational constants (B_{v^+}, D_{v^+}, B_e, and α_e), and the vibrational energy spacings $\Delta G(v^++1/2)$ for $H_2^+(X^2\Sigma_g^+, v^+=0\text{-}18)$ are determined. With a significantly higher photoelectron energy resolution achieved in the present study, the precisions of these spectroscopic values are higher than those obtained in the previous photoelectron studies. As expected, the spectroscopic results for $H_2^+(X^2\Sigma_g^+, v^+=0\text{-}18)$ derived from this VUV-PFI-PE study are in excellent agreement with high-level theoretical predictions.

Key words: H_2, Rotationally resolved, Vacuum ultraviolet, Pulsed field ionization, Photoelectron, Buckingham-Orr-Sichel, Spectrum simulation

I. INTRODUCTION

As the simplest cationic molecular system, the potential energy surfaces and rovibrational level energies of $H_2^+/HD^+/D_2^+$ in their ground states can be calculated [1-8] with higher accuracy than experimental measurements [1,4,9-15]. For this reason, detailed experimental and theoretical studies of these cations have served to provide valuable information concerning the accuracy of different quantum mechanical formulations for molecular structure calculations, such as the Born-Oppenheimer, adiabatic, and nonadiabatic solutions [1]. The absence of interelectron interactions also allows other aspects of molecular structure theories to be investigated. The accuracy of bound rovibrational state energies and thus, the dissociation energies of $H_2^+/HD^+/D_2^+$ calculated by the nonadiabatic procedures with relativistic and radiative corrections was believed to be 0.0001 cm^{-1} [1,4,7].

Since homonuclear diatomic ions, such as H_2^+ and D_2^+, do not possess electric dipole moments, rovibrational transitions involving these ions are electric dipole-disallowed. As a result, the spectroscopic properties for H_2^+ and D_2^+ can be calculated much easier than measured by traditional spectroscopic methods. Most of the previous experimental knowledge of H_2^+ and its isotope species has come from indirect spectroscopic measurements, such as photoionization efficiency (PIE), photoelectron, and Rydberg series studies of H_2 [9-19]. Although the resolutions of photoelectron [9-17] measurements are lower than those of other spectroscopic techniques [1,4], such as the ion-beam [20,21] and radiofrequency [22] measurements, photoelectron methods [11,16,21] have a distinct advantage over these other spectroscopic techniques, allowing the examination of nearly all the vibrational bands [17] of a diatomic ion.

In addition to obtaining spectroscopic information for H_2^+, a primary motivation for high-resolution PIE and photoelectron studies of H_2 concerns the fundamental understanding of molecular photoionization dynamics [9-19]. The vacuum ultraviolet (VUV) PIE spectrum of H_2 near its ionization threshold in the region of 15.3-17.0 eV is overwhelmingly dominated by autoionizing Rydberg structures [18,19]. The majority of these Ry-

†Part of the special issue "Cun-hao Zhang Festschrift".
*Author to whom correspondence should be addressed. E-mail: cyng@chem.ucdavis.edu

dberg features has been analyzed based on the multichannel quantum defect theory (MQDT) [14,23,24]. Due to the large rotational constants for H_2 and H_2^+, partially rotational-resolved photoelectron spectra for H_2 have been observed previously using the NeI [9] and HeI [10,11] photoelectron spectroscopic techniques. The molecular beam HeI photoelectron measurements of Pollard *et al.* achieved a photoelectron energy resolution of 90-100 cm^{-1} (full-width at half-maximum, FWHM) [11], allowing the identification of the vibrational bands of $H_2^+(X^2\Sigma_g^+, v^+=0\text{-}18)$. However, despite of the large rotational and vibrational constants of H_2 and H_2^+, the energy resolution attained in the latter HeI photoelectron study did not allow the observation of well resolved rotational structures.

The advent of VUV laser [17,25,26] and VUV synchrotron [27-31] pulsed field ionization-photoelectron (PFI-PE) spectroscopic techniques has made possible the measurement of fully rotationally resolved photoelectron vibrational bands of $H_2^+(X^2\Sigma_g^+)$ [12,15] and $HD^+(X^2\Sigma_g^+)$ [16]. Using the VUV laser PFI-PE technique, Merkt and Softley have obtained a fully rotationally resolved photoelectron vibrational band for $H_2^+(X^2\Sigma_g^+, v^+=2)$ [12]. The couplings between high-n (n>100) Rydberg (pseudocontinuum) states, lying at a few wavenumbers below an ionization limit, and low-n Rydberg (interloper) states in near-energy resonance with the pseudocontinuum states are expected to have a significant effect on the observed VUV-PFI-PE intensities [14,23,24]. Hence, the rotational components of the PFI-PE vibrational band should exhibit different intensities compared to those resolved in a HeI photoelectron study, where perturbations due to near-resonance autoionization seldom occur. The relative intensities of rotational photoionization transitions observed in the VUV-PFI-PE band of $H_2^+(X^2\Sigma_g^+, v^+=2)$ have been simulated using the MQDT, the result of which confirms the near-resonance perturbation mechanism [14].

Although VUV laser radiation with useful intensities can now be readily generated up to 19.5 eV by four-wave mixing schemes using commercial pulsed dye lasers, the tunability of such VUV laser sources over a broad energy range of several eV remains a nontrivial task [17,25,26]. In term of the ease of tunability covering a broad VUV energy range, the use of monochromatized VUV synchrotron radiation [27-29] has a great advantage over VUV laser sources. By employing the broadly tunable high-resolution monochromatized VUV synchrotron source associated with the Chemical Dynamics Beamline at the Advanced Light Source (ALS), together with the synchrotron based PFI-PE detection [30,31] scheme, we have obtained rotationally resolved PFI-PE spectra for many simple molecules in the VUV energy range of 9-25 eV [17,27]. For H_2, HD, and D_2, fully rotationally resolved PFI-PE vibrational bands for H_2^+, HD^+, and D_2^+ have been recorded using the VUV synchrotron [21] based PFI-PE method in the energy range of 15.30-18.15 eV, covering the formation of v^+ levels up to near the dissociation limits of these cations. A preliminary report on the analysis of selected VUV-PFI-PE vibrational bands for $H_2^+(X^2\Sigma_g^+, v^+=0, 2, 6, 9, \text{and } 11)$ thus measured has been communicated [15]. This paper presents the analysis of the full VUV-PFI-PE spectrum of H_2, including the assignment of observed rovibrational photoionization transitions $H_2^+(X^2\Sigma_g^+, v^+=0\text{-}18, N^+=0\text{-}5) \leftarrow H_2(X^1\Sigma_g^+, v''=0, J''=0\text{-}4)$ and the simulation of their relative intensities based on the Buckingham-Orr-Sichel (BOS) model [32]. Although the BOS model does not take into consideration interchannel couplings, and thus cannot account for the near resonance autoionizing perturbation, the comparison of the experimental PFI-PE bands with BOS simulations has helped to assess the degree of perturbation by the near resonance autoionizing mechanism to the rotational transitions resolved in the VUV-PFI-PE measurements [15,16].

II. EXPERIMENTS

The present experiment was performed using the high resolution VUV facility and the photoion-photoelectron apparatus of the Chemical Dynamic Beamline at the ALS [28-31]. Since the experimental arrangement and procedures have been described in detail previously, only a brief account is given here. Helium was used in the harmonic gas filter where higher undulator harmonics with photon energies greater than 24.59 eV were suppressed. The fundamental light from the undulator was dispersed by the 6.65 m monochromator equipped with an Os coated 4800 L/mm grating (dispersion=0.32 Å/mm). Monochromator entrance/exit slits of 100/100 μm (wavelength resolution=0.032 Å (FWHM)) and 150/150 μm (wavelength resolution of 0.048 Å (FWHM)) were used for the measurement of the v^+=0-14 and v^+=15-18 vibrational bands, respectively.

Both a continuous molecular beam and an effusive beam of pure H_2 were used in this experiment. The continuous molecular beam was produced by supersonic expansion through a stainless steel nozzle (diameter=0.127 mm) at a stagnation pressure of 43.9 kPa and a nozzle temperature of 298 K. The molecular beam was skimmed by a conical skimmer (diameter=1 mm) before intersecting the monochromatized VUV light beam 7 cm downstream at the photoionization region. The rotational temperature was found to be ≈265 K for the H_2 molecular beam sample. The H_2 effusive beam was introduced into the photoionization region through a metal orifice (diameter=0.5 mm) at room temperature and 0.5 cm from the photoionization region. The rotational temperature was 298 K for the effusive beam.

The ALS storage ring is capable of filling 328 electron buckets in a period of 656 ns. Each electron bucket emits a light pulse of 50 ps with a time separation of 2 ns between successive bunches. In each storage ring

DOI:10.1088/1674-0068/20/04/352-364

period, a dark-gap (48 or 60 ns) consisting of 24 or 30 consecutive unfilled buckets exists for the ejection of cations from the orbit. Thus, the present experiment [30,31] is performed in the multibunch mode with 304 or 298 bunches in the synchrotron orbit, corresponding to a repetition rate of 464 or 454 MHz. A pulsed electric field of 0.67 V/cm (width=40 ns) was applied to the repeller at the photoionization region for measurements of the PFI-PE bands for $H_2^+(v^+$=0-9), while the PFI-PE bands for $H_2^+(v^+$=10-18) were measured using a pulsed field of 1.2 V/cm (width=40 ns). In addition to field ionize high-n ($n\geq$100) Rydberg states, the PFI field applied to the repeller at the photoionization region also serves to extract photoelectrons into the electron spectrometer. The PFI field was applied every 1 ring period (0.656 μs) for vibrational levels v^+=10-18, and delayed by 20 ns with respect to the beginning of a 60 ns dark-gap. For vibrational levels v^+=0-9, the pulsed electric field was applied every 2 ring periods (1.31 μs) and delayed by 8 ns with respect to the beginning of a 48-ns dark-gap. The electron spectrometer, which consists of a steradiancy analyzer and a hemispherical energy analyzer arranged in tandem, is used to filter prompt electrons [31]. Judging from the width of the rotational transitions observed, we concluded that the PFI-PE energy resolution achieved in the present experiment is 6-8 cm^{-1} (FWHM), which is comparable to the VUV photon energy resolution [28,30,31]. We estimated that the suppression factor is $\approx 5\times10^{-4}$ for prompt electrons with kinetic energies of 4.5 meV. The suppression factor should be smaller than 5×10^{-4} for autoionizing levels lying at energies greater than 4.5 meV with respect to an ionization threshold. The absolute photon energy scales for the H_2 spectra were calibrated using the $Ne^+(^2P_{3/2})$ and $Ar^+(^2P_{3/2})$ PFI-PE bands measured in the same experimental conditions [28-31]. In the present experiment, the photon energy step size used is ≈0.2 meV (1.6 cm^{-1}). The dwell time at individual steps is in the range of 2-40 s.

III. RESULTS AND DISCUSSION

A. Assignment of rovibronic transitions

For the one-photon ionization process $H_2^+(X^2\Sigma_g^+,\ v^+,\ N^+)\leftarrow H_2(X^1\Sigma_g^+,\ v''=0,\ J'')$, the total wavefunction for the neutral and ion $|\Psi\rangle=|\psi_{el}\chi_{vib}\chi_{rot}\psi_{nucl.spin}\rangle$ must be antisymmetric under the space-fixed nuclear exchange operation X_N because H_2 nuclei are fermions. The vibrational state $|\chi_{vib}\rangle$ is not affected by the exchange operator since it only depends on the internuclear distance. The exchange symmetry of $|\psi_{el}\chi_{rot}\rangle$ under X_N is given by

$$\begin{aligned} X_N|\psi_{el}\chi_{rot}\rangle &= i_1 i_2|\psi_{el}\chi_{rot}\rangle \\ &= [(-1)^J(+)][+]|\psi_{el}\chi_{rot}\rangle \\ &= (-1)^J|\psi_{el}\chi_{rot}\rangle \end{aligned} \quad (1)$$

where i_1 represents inversion of all particles through the origin and i_2 represents inversion of electrons through the origin. This results in $|\psi_{el}\chi_{rot}\rangle$ being antisymmetric for odd J and symmetric for even J. The effect of X_N on the nuclear spin function $|\psi_{nucl.spin}\rangle$ for a homonuclear diatomic molecule with $(2I+1)^2$ nuclear spin states results in $(2I+1)(I+1)$ symmetric spin states and $(2I+1)I$ antisymmetric spin states, where I is the spin of the nucleus. For H_2, I=1/2, and this results in three symmetric and one antisymmetric nuclear spin states.

Since the rovibronic transitions in this experiment involve photoionization, we must take into account the angular momentum coupling of the neutral, ion, and ejected electron. For direct photoionization of H_2, the angular momentum coupling factor Q can be considered as a Hund's case b←b transition, which is expressed as [32]

$$Q(\lambda, N^+, N'') = (2N^+ + 1)\begin{pmatrix} N^+ & \lambda & N'' \\ -\Lambda^+ & \Delta\Lambda & \Lambda'' \end{pmatrix}^2 \quad (2)$$

where $\Delta\Lambda$ is the difference in orbital angular momenta between the ion and the neutral, and the rotational angular momenta of the ion and neutral are represented by N^+ and N'', respectively. The properties of Eq.(2) are such that given Λ^+=0 and Λ''=0, Eq.(2) will vanish if N^++N''+λ is odd. The general interpretation of λ is the angular momentum transferred to the ejected electron in the photoionization process. The values of λ are constrained by the triangular condition $\Delta N\leq\lambda\leq N^+ + N''$. An additional constraint on λ is $\lambda=|l-1|,\ldots,|l+1|$, which is due to the dipole selection rule. Here, l is the angular momentum of the ejected photoelectron.

The parity selection rule connecting rovibronic states of the neutral and ion is given by [32-34]

$$\triangle J + \triangle S + \triangle p + l = \text{even} \quad (3)$$

where $\triangle J=J^+-J''$, $\triangle S=S^+-S''$ is the difference in total spin between the ion and neutral, and $\triangle p$ represents the change in Kronig parity of the initial and final states (p=0 for Λ^+ or 1 for Λ^-). For a $^2\Sigma_g^+\leftarrow{}^1\Sigma_g^+$ transition, $\triangle S$=1/2, $\triangle p$=0, and $\triangle J=\triangle N+\triangle S$ (for Hund's case b←b). Eq.(3) thus reduced to $\triangle N+l$=odd. Since l must be odd for a g←g transition in order for the matrix element $\langle\Psi_{ion}|\langle\Psi_{photoelectron}|\mu|\Psi_{mol}\rangle$ not to vanish, $\triangle N$ is required to be even (0, ±2, ±4,...). As shown previously [15], only the $\triangle N$=0 and ±2 transitions were observed in this experiment. The partial waves of the ejected photoelectron are l=1 and 3 for λ=2, and l=1 for λ=0. This means that the Q-branch gains intensity through the excitation of a s- and a d-wave electron, with the majority coming from the s-wave electron. However, the O- and S-branches gain intensity only from the excitation of a d-wave electron. This is due to the constraint on the λ value introduced by the triangular condition.

DOI:10.1088/1674-0068/20/04/352-364

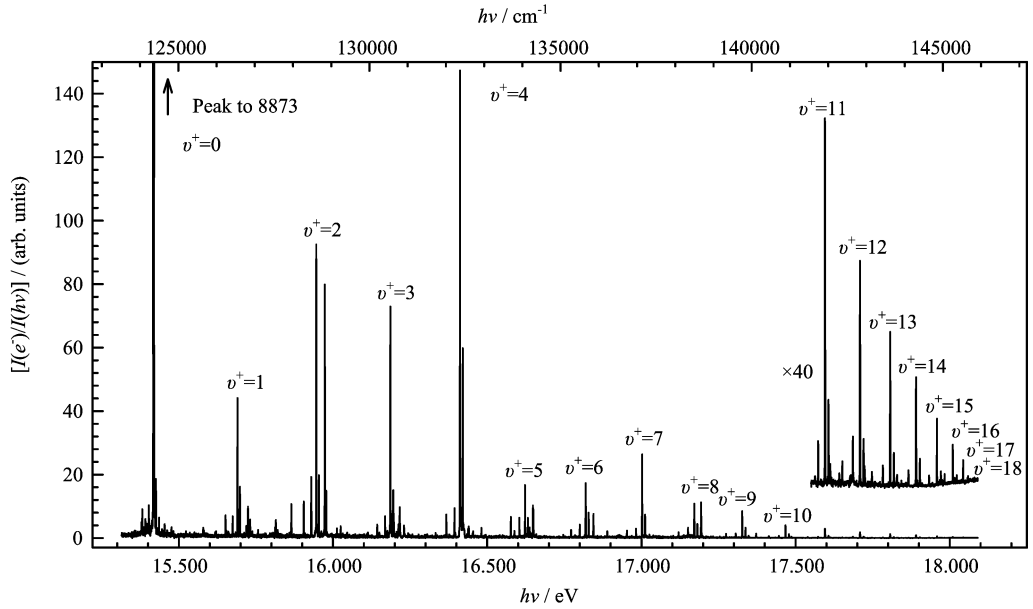

FIG. 1 Rotationally resolved VUV PFI-PE spectrum of H_2 in the energy range of 15.30-18.09 eV, covering the ionization transitions $H_2^+(X^2\Sigma_g^+, v^+=0\text{-}18, N^+) \leftarrow H_2(X^1\Sigma_g^+, v''=0, J'')$. Note that the relative intensity for the (1,1) transition of $v^+=0$ is to 8873.

The complete rotationally resolved VUV-PFI-PE spectrum for H_2 in the photon energy range of 15.3-18.11 eV, covering the vibrational bands for $H_2^+(X^2\Sigma_g^+, v^+=0\text{-}18)$ is shown in Fig.1. The individual PFI-PE vibrational bands for $H_2^+(X^2\Sigma_g^+, v^+=0\text{-}18)$ are shown in Figs.2(a)-(s), respectively. The rotational assignments (N^+, J'') with $N^+=0\text{-}5$ and $J''=0\text{-}4$ of individual vibrational bands are marked on top of these figures. In order to compare the relative intensities of these vibrational bands, the vertical $I(e^-)/I(h\nu)$ scales for Figs.2(a)-(s) have the same units, where $I(e^-)$ and $I(h\nu)$ represent the PFI-PE intensity and the VUV photon intensity, respectively. Using the spectroscopic constants for H_2 obtained from Refs.[13] and [35], the rotational level energies for $v''=0$, $J''=0\text{-}10$ were calculated. The rotation-vibration energy levels for H_2^+ were taken from theoretical calculations by Hunter, Yau, and Pritchard (HYP) [2], Wolniewicz and Poll (WP) [5], and Moss [7]. Among these calculations, the nonadiabatic predictions of Moss [7], which have taken into account the relativitic, and radiative corrections, are believed to be the most accurate with error limits of 0.0001 cm^{-1} [7]. Combining the rovibronic level energies of H_2 and H_2^+, together with the known ionization energy [13] of H_2 allowed the calculation of the rovibronic transitions, $H_2^+(X^2\Sigma_g^+, v^+=0\text{-}18, N^+=0\text{-}10) \leftarrow H_2(X^1\Sigma_g^+, v''=0, J''=0\text{-}10)$, which were used to assign the rovibronic transitions observed in this experiment. We found that the ionization energies thus calculated for the ionization transitions $H_2^+(X^2\Sigma_g^+, v^+=0\text{-}18, N^+=0\text{-}10) \leftarrow H_2(X^1\Sigma_g^+, v''=0, J''=0)$, i.e., $(N^+,J'')=(0,0)$ and positions of other (N^+,J'') rotational lines are in excellent agreement with those observed in the present VUV-PFI-PE spectrum of H_2 with the maximum deviation of $\leq$0.5 meV.

Since the cross section for direct photoionization is very low compared to that for autoionization in H_2 [21,22], a suppression factor [31] of 5×10^{-4} for prompt electrons achieved in the present experiment is not sufficient to completely suppress structures originating from strong autoionization states in the PFI-PE spectrum. Photoionization of H_2 has been used as a model system for the detailed experimental and theoretical investigation of the near-resonance autoionization mechanism [12,16,20,21]. The experiment [12] and theoretical [24] simulation of the VUV-PFI-PE band for $H_2^+(X^2\Sigma_g^+, v^+=2)$ using MQDT shows unambiguously that the couplings of high-n Rydberg pseudocontinuum states and near-resonance interloper states converging to higher ionization thresholds have a significant effect on the VUV-PFI-PE intensities of rotational transitions. An interesting example revealing this effect is the (1,1) line of the $v^+=0$ band, i.e., the strongest peak shown in Fig.1 or Fig.2(a). This transition is overwhelmingly the most intense peak observed in the entire VUV-PFI-PE spectrum with an electron counting rate of $>5\times10^4$ counts/s and is $\approx$500 times higher than that of the (0,0) peak of the $v^+=0$ band. The high intensity for this (1,1) line is due to the fact the $H_2^+(X^2\Sigma_g^+, v^+=0, N^+=1)$ ionization threshold nearly coincides with a very strong autoionizing resonance of H_2 [21,22].

Photoelectron peaks resolved in the VUV-PFI-PE spectrum of Fig.1, which cannot be assigned to (N^+,J'') ionization thresholds, are attributed to prompt electron

DOI:10.1088/1674-0068/20/04/352-364

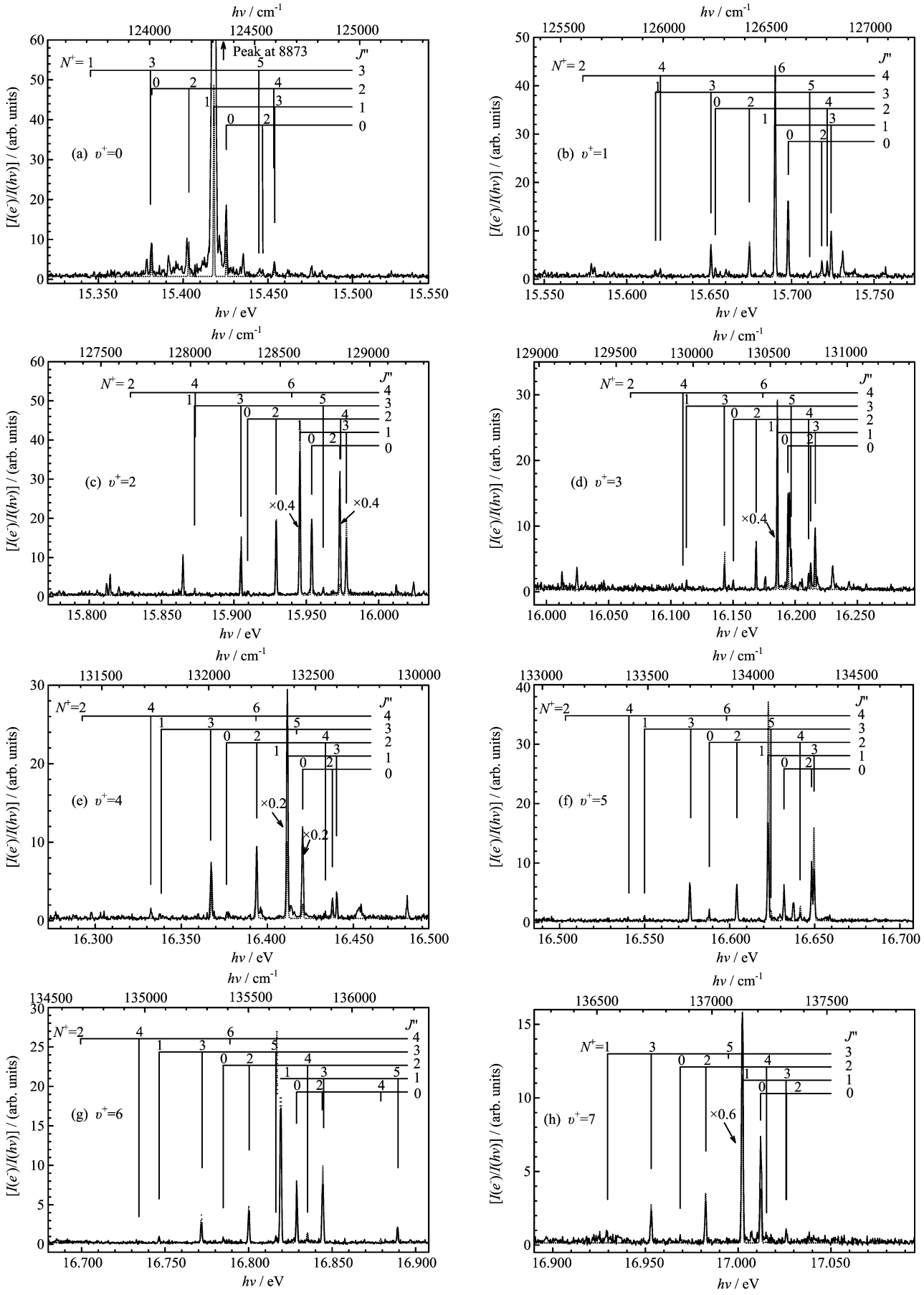

DOI:10.1088/1674-0068/20/04/352-364

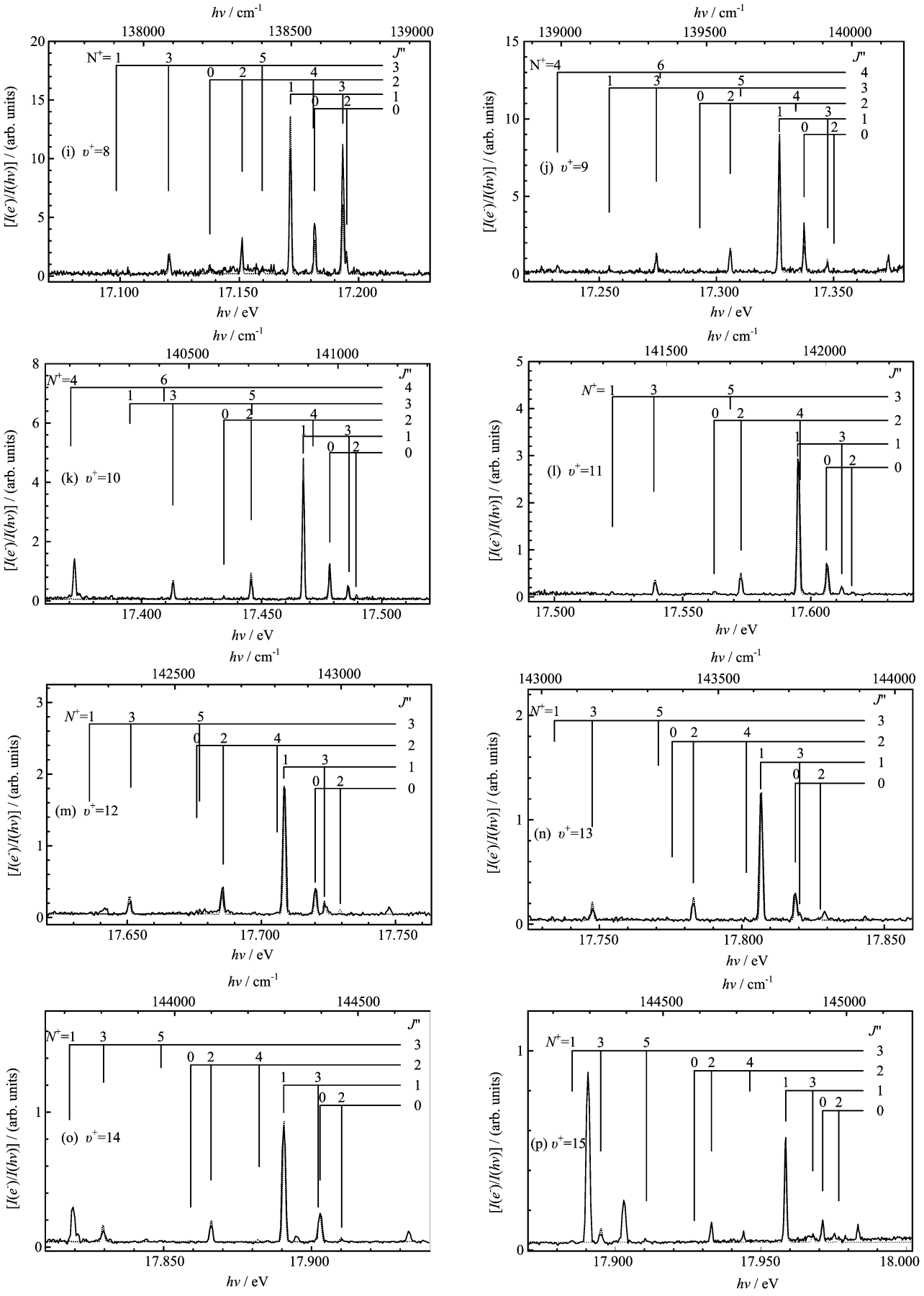

DOI:10.1088/1674-0068/20/04/352-364

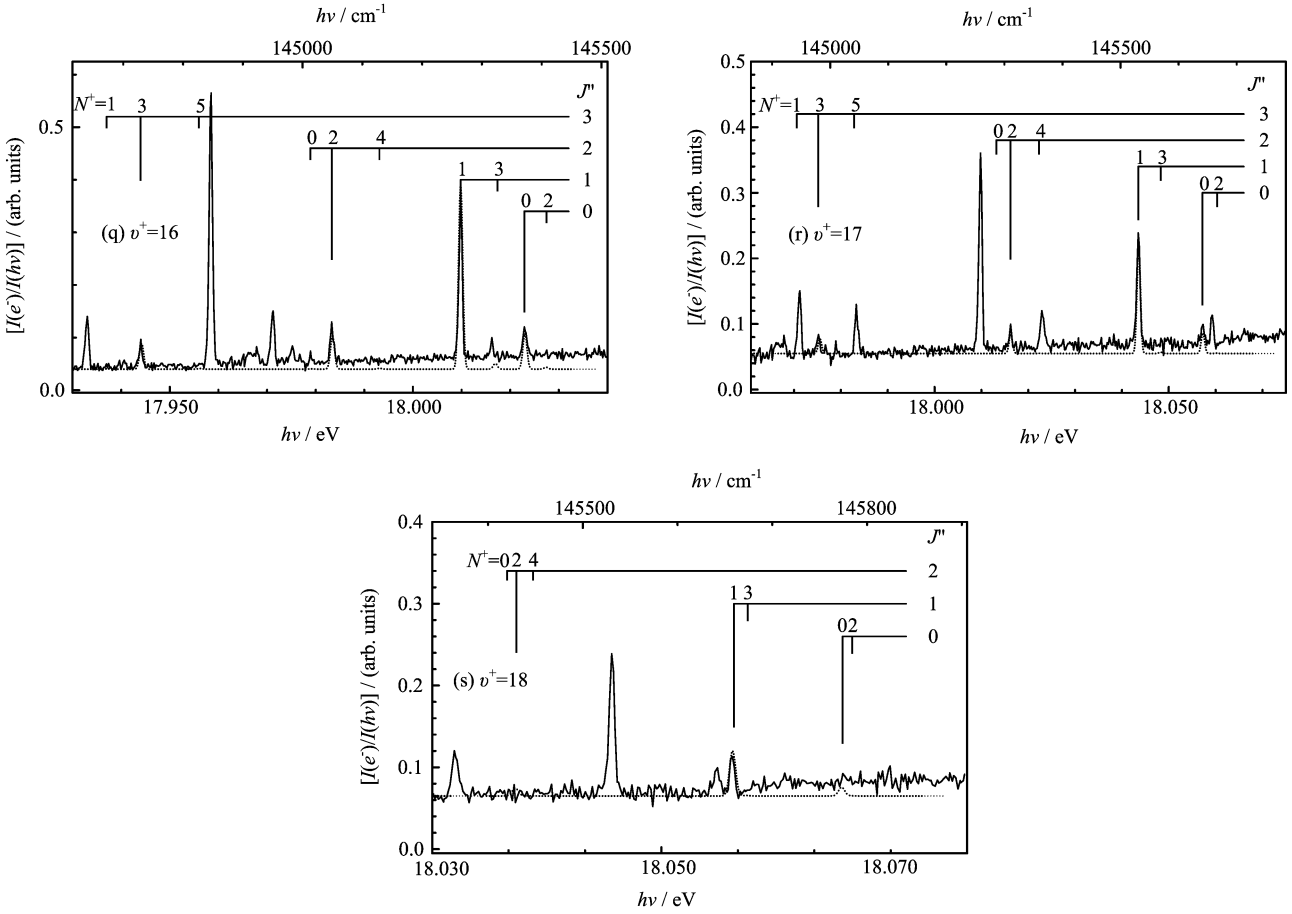

FIG. 2 VUV-PFI-PE vibrational bands for $H_2^+(X^2\Sigma_g^+,\ v^+=0\text{-}18)$ are shown in (a)-(s), respectively. The BOS fits are depicted by the dashed curves. All spectra have the same units of $I(e^-)/I(h\nu)$. Note that the relative intensity for the (1,1) transition of $v^+=0$ is to 8873.

background features from autoionizing Rydberg levels of H_2 [18,19]. The contamination by near resonance autoionizing states is most serious for the $v^+=0$ PFI-PE vibrational band obtained in the present experiment using the hemispherical energy analyzer as the PFI-PE detector. The contamination by prompt electron peaks is expected to be less serious at higher v^+ states because strong autoionizing Rydberg states are mostly concentrated in the energy range (≈15.3-16.7 eV) covering the lower $HD^+(v^+\leq 5)$ states [18,19]. This expectation is confirmed by the VUV-PFI-PE vibrational bands for $H_2^+(X^2\Sigma_g^+,\ v^+=0\text{-}5)$ (Figs.2 (a)-(f)), where many near-resonance autoionization peaks can be identified, whereas the PFI-PE bands for $v^+=6\text{-}18$ (Figs.2 (g)-(s)) are nearly free from autoionization features. Although many autoionizing Rydberg peaks resolved in the VUV-PIE spectrum [18,19] of H_2 can be identified as minor background electron peaks in the VUV-PFI-PE bands for $H_2^+(X^2\Sigma_g^+,\ v^+=0\text{-}5)$ obtained in the present study, the relative intensities for these background electron peaks are not in proportion with the relative intensities of the autoionization Ryberg peaks resolved in the PIE spectrum.

B. Rotational line intensities

As indicated above, H_2 is introduced into the photoionization region both in the form of a molecular beam and an effusive beam at 298 K. We have compared the PFI-PE spectra recorded using the H_2 supersonic beam with those obtained using the effusive H_2 beam. On the basis of this comparison, we concluded that the rotational temperature for the H_2 molecular beam is ≈265 K [15]. Since ortho-hydrogen (odd J'') and para-hydrogen (even J'') exist in the ratio of 3:1, we estimated the rotational population ratios for $(J''=0):(J''=1):(J''=2):(J''=3):(J''=4):(J''=5)$ to be 0.1447:0.6842:0.1049:0.0639:0.0021:0.0003 at 265 K for the molecular beam and 0.1301:0.6605:0.1168:0.0880:0.0038:0.0008 at 298 K for the effusive beam. The rotational transition intensities are expected to roughly reflect the thermal distribution of rotational levels at such a temperature if the near-resonance autoionization mechanism does not play a role in the production PFI-PEs.

As shown in the VUV-PFI-PE vibrational bands for $H_2^+(X^2\Sigma_g^+,\ v^+=0\text{-}18)$, the dominant rotational tran-

DOI:10.1088/1674-0068/20/04/352-364

sitions are (0,0), (1,1), (2,2), and (3,3). In general, the PFI-PE intensity for (1,1) is higher than that for (0,0) within a given vibrational band. This observation and the low PFI-PE intensities for transitions involving $J''\geq 4$ are in general accord with the thermal J'' distribution of H_2. Weak transitions attributable to $\triangle N=\pm 2$, i.e., (2,0), (3,1), (0,2), (4,2), (1,3), and (5,3) are also observed. The dominance of the rotational transitions with $\triangle N=0$ over that with $\triangle N=\pm 2$ is consistent with the results of previous experiments [9-12,15] and theoretical [2] predictions.

C. Spectral simulation

The Buckingham-Orr-Sichel (BOS) model [32] is described by the formula

$$\sigma(N^+ \leftarrow N^{''}) \propto \sum_{\lambda} Q\left(\lambda, N^+, N''\right) C_\lambda \qquad (4)$$

This model was derived to predict rotational line strength $\sigma(N^+\leftarrow N'')$ observed in one photon direct ionization of diatomic molecules. Since the BOS model does not take into account of any interchannel couplings, the BOS simulation is not expected to be able to reproduce the intensities of rotational transitions resolved in a PFI-PE vibrational band of H_2 if strong perturbation by near resonance autoionization Rydberg states occurs. Nevertheless, the comparison of the experimental rotational PFI-PE intensities with those of the BOS simulation would reveal the importance of the near resonance autoionizing mechanism. According to Eq.(4), the rotational line strength is separated into two factors. The factor C_λ is associated with the electronic transition moments, which is the linear combination of electron transition amplitudes for the possible angular momenta l of the ejected electron. The general interpretation of λ is that of the angular momentum transferred in the photoionization process. The other factor Q is determined by the standard angular momentum coupling constants (i.e., Clebsch Gordon coefficients), which were calculated using the formula for a Hund's case b←b transition in the present study as given by Eq.(2). The known spectroscopic constants for the $H_2(X^1\Sigma_g^+, v''=0)$ ground state were used. The best BOS fits of the VUV-PFI-PE bands for $H_2^+(X^2\Sigma_g^+, v^+=1\text{-}18)$ are depicted as dashed curves in Figs.2 (a)-(s). The fact that only the $\triangle N=0$ and ± 2 rotational branches are observed implies that only the BOS coefficients C_0 and C_2 are nonzero. The C_0 and C_2 values for the BOS simulated spectra of $v^+=0\text{-}18$ are listed in Table I. The dominance of the $\triangle N=0$ or Q-branch observed in the experimental spectra is consistent with the significantly higher C_0 values than the corresponding C_2 values. As expected, the BOS simulation, which does not take into account the effect of near-resonance autoionization, cannot account for the overwhelming intensity for the (1,1) transition observed in the $v^+=0$ PFI-PE band.

TABLE I BOS coefficients C_0 and C_2 for the best fits of theVUV-PFI-PE vibrational bands for $H_2^+(X^2\Sigma_g^+, v^+=0\text{-}18)$. The sum of C_0 and C_2 for a given v^+ state is arbitrarily normalized to 100

v^+	C_0	C_2	v^+	C_0	C_2
0	90	10	10	85	15
1	70	30	11	90	10
2	75	25	12	85	15
3	70	30	13	90	10
4	90	10	14	85	15
5	50	50	15	90	10
6	60	40	16	95	5
7	95	5	17	98	2
8	50	50	18	98	2
9	85	15			

Many weak structures observed in the $v^+=0$ VUV-PFI-PE vibrational band cannot be assigned to rotational transitions. These weak structures can be attributed to contamination from near resonance autoionizing Rydberg states. By employing a wider synchrotron dark-gap (104 ns) and the time-of-flight selection scheme [36], we have achieved a higher suppression factor for prompt electrons than that attained in the present study by using a hemispherical energy analyzer [28-31]. Figures 3 (a) and (b) [36] depict the $v^+=0$ PFI-PE vibrational band measured using the TOF selection scheme and that of the present study, respectively. This comparison clearly identifies many background features originating from autoionizing Rydberg levels in the $v^+=0$ PFI-PE band observed in this study, as they are not observed in the spectrum measured using the TOF selection scheme. Contaminations originating from near resonance autoionizing states are surprisingly minor for other PFI-PE vibrational bands. General agreement is found between the experimental spectra and the BOS simulation of PFI-PE vibrational bands for $v^+\geq 1$. In general, the agreement becomes better for higher vibrational levels. Disregarding the C_0 and C_2 values for the $v^+=0$ band, we find that the C_0 value in general increases compared to the C_2 value with increasing v^+. Such a trend is consistent with the experimental observation that the $\triangle N=\pm 2$ rotational branch diminishes as v^+ is increased.

The intensities for the rotational transitions, (N^+,J''), $J''=0\text{-}3$ and $N^+=0\text{-}5$, associated with the $v^+=0$, 1, 2, 5, and 8 bands have been calculated by Itikawa [37] at photoionization wavelengths of 584 Å HeI and 736 Å NeI. These calculations, which have not taken into account the coupling of interloper states, are in qualitative agreement with the HeI [10,11] and NeI [9] results. A careful comparison of the experimental VUV-PFI-PE, HeI, and NeI studies and the previous theoretical results for the $v^+=2$ vibrational band has been made by Softley and co-workers [12,24]. These

DOI:10.1088/1674-0068/20/04/352-364

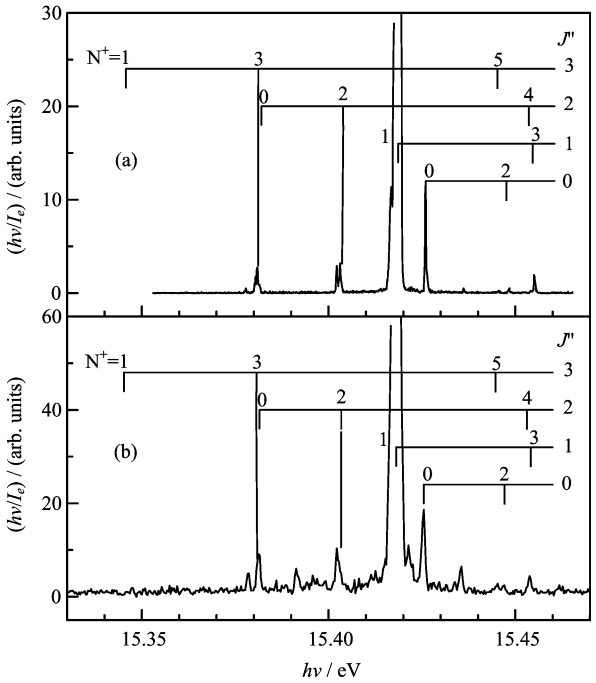

FIG. 3 VUV-PFI-PE spectra for the $H_2^+(X^2\Sigma_g^+,\ v^+=0)$ origin band observed using the (a) dark-gap TOF selection scheme and (b) hemispherical energy analyzer for PFI-PE detection [36].

experimental and theoretical intensities for rotational photoionization transitions have also been compared with the VUV-PFI-PE results and the BOS simulation of this study [15]. Note that the BOS simulation for the v^+=2 band accounts well for all the relative rotational intensities except that for the (2,0) transition. The relatively VUV-PFI-PE intensities observed here for the v^+=2 band are in reasonable agreement with those [12] of Merkt and Softley [15].

Another important factor that could affect the PFI-PE intensities is the effective lifetime for high-n Rydberg states involved in the VUV-PFI-PE measurements. If the effective lifetime is shorter than the time interval for adjacent Stark field pulses, the measured PFI-PE intensity would be lower than the actual threshold photoelectron intensity. We have examined several VUV-PFI-PE bands obtained at time intervals of 0.656, 1.31, 1.97 μs, corresponding to the times of applying the Stark field pulse every one, two, and three synchrotron ring periods, respectively. Since the relative rotational intensities observed in the one, two, and three period operations were in agreement with experimental uncertainties, we concluded that the rotational intensities resolved in the VUV-PFI-PE bands of the present study were not influenced by the Rydberg lifetime effect.

The comparison of the BOS simulated spectra with the PFI-PE vibrational bands in Figs.2 (a)-(s) shows that perturbations of the PFI-PE intensities for rotational transitions by near resonance autoionizing Rydberg states are only important for the v^+<6 bands. Thus, the rotationally resolved PFI-PE bands for $H^{2+}(v^+\geq 6)$ provide reliable estimates of state-to-state cross sections for direct photoionization of H_2, which can be used for benchmarking future photoionization dynamics calculations. Considering that the autoionizing Rydberg levels for H_2 at energies near its ionization threshold have been well analyzed, the rotationally resolved PFI-PE bands for $H_2^+(v^+\leq 6)$ obtained with well defined PFI conditions represent valuable data for fundamental understanding of the near resonance autoionizing mechanism. It is our hope the PFI-PE bands for $H_2^+(v^+<6)$ presented here would stimulate a rigorous simulation by the MQDT.

D. Vibrational and rotational energy levels

The vibrational energy levels are fitted to the equation

$$G(v^+) = \omega_e\left(v^+ + \frac{1}{2}\right) - \omega_e\chi_e\left(v^+ + \frac{1}{2}\right)^2 + \omega_e y_e\left(v^+ + \frac{1}{2}\right)^3 + \omega_e z_e\left(v^+ + \frac{1}{2}\right)^4 \quad (5)$$

The vibrational constants, ω_e, $\omega_e\chi_e$, $\omega_e y_e$, and $\omega_e z_e$ for H_2^+ were determined by fitting the experimental VUV-PFI-PE vibrational energy level spacings according to the equation: $\triangle G(v^+{+}1/2){=}G(v^+{+}1){-}G(v^+)$. The vibrational spacings $\triangle G(v^+{+}1/2)$ for v^+=0-17 determined in the present study are listed in Table II to compare with the previous HeI experimental results of Pollard *et al.* [11] and the theoretical predictions [2,3,5,7] of HYP, WP and Moss. The present VUV-PFI-PE vibrational spacings are in good agreement with the HeI results as well as these theoretical predictions. The predictions of Moss and WP on vibrational spacings are essentially the same with discrepancies less than 0.01 cm^{-1}; but with higher accuracy than the HYP values, which are slightly higher and lower than the Moss values for v^+<10 and v^+>10, respectively. The discrepancies between the VUV-PFI-PE experimental vibrational spacings and the corresponding theoretical predictions of Moss are shown in parentheses next to the VUV-PFI-PE values in Table II, which are found to be in the range of +3.5 to −1.2 cm^{-1}. These discrepancies correspond to the average deviation of 0.1±1.3 cm^{-1}. The latter standard deviation of 1.3 cm^{-1} can be taken to be a good estimate of the uncertainty for the experimental vibrational spacings determined in this study. Since independent energy calibrations were made for individual PFI-PE vibrational bands, these discrepancies observed for the vibrational spacings reflect the accuracy of the energy calibration procedures used in the VUV synchrotron based PFI-PE measurement. The plots of $\triangle G(v^+{+}1/2)$ versus $(v^+{+}1/2)$ obtained by the present PFI-PE measurement and the Moss calculation

DOI:10.1088/1674-0068/20/04/352-364

TABLE II Comparison of the vibrational spacings $\triangle G(v^+{+}1/2)$ in cm^{-1} for the $H_2^+(X^2\Sigma_g^+)$ ground state obtained by experimental measurements and theoretical predictions

$v^+{+}1/2$	VUV-PFI-PE[a]	HeI[b]	HYP[c]	WP[d]	Moss[e]
0.5	2194.63 (3.50)	2190.9	2191.32	2191.13	2191.1266
1.5	2066.12 (2.21)	2065.2	2064.09	2063.91	2063.9140
2.5	1941.19 (0.27)	1941.8	1941.08	1940.92	1940.9244
3.5	1820.69 (−0.81)	1822.1	1821.64	1821.50	1821.4993
4.5	1703.78 (−1.22)	1706.2	1705.13	1705.00	1704.9979
5.5	1589.63 (−1.16)	1591.1	1590.90	1590.79	1590.7869
6.5	1477.40 (−0.83)	1477.7	1478.32	1478.23	1478.2301
7.5	1366.28 (−0.40)	1367.0	1366.75	1366.68	1366.6781
8.5	1255.42 (−0.04)	1257.8	1255.51	1255.46	1255.4562
9.5	1143.99 (0.14)	1145.8	1143.88	1143.85	1143.8508
10.5	1031.17 (0.08)	1031.9	1031.09	1031.09	1031.0927
11.5	916.12 (−0.22)	913.3	916.31	916.34	916.3396
12.5	798.02 (−0.63)	796.6	798.59	798.65	798.6528
13.5	676.02 (−0.96)	676.4	676.86	676.98	676.9760
14.5	549.31 (−0.81)	548.4	549.97	550.12	550.1228
15.5	417.04 (0.19)	415.4	416.62	416.84	416.8362
16.5	278.40 (2.2)	280.3	275.96	276.25	276.2424
17.5	132.54 (1.0)	—	131.26	131.58	131.5798

[a] Experiment. This work.
[b] Experiment. Ref.[11].
[c] Theory. Ref.[2].
[d] Theory. Ref.[5].
[d] Theory. Ref.[7].

are shown in Fig.4. Both curves show a positive curvature at low $(v^+{+}1/2)$ and a negative curvature at high $(v^+{+}1/2)$ with a point of inflection at $\approx 7\frac{1}{2}$, as was observed in the HeI photoelectron study [11]. The sum of VUV-PFI-PE $\triangle G(v^+{+}1/2)$ values for v^+=0-17 gives 21357.75 cm^{-1} which is found to be higher than the sum of Moss theoretical prediction by 2.4 cm^{-1}. This experimental sum is about 22 cm^{-1} lower than the predicted dissociation energy [7] of 21379.3501 cm^{-1} for $H_2^+(X^2\Sigma_g^+)$ based on the Moss nonadiabatic calculation.

The vibrational constants ω_e, $\omega_e\chi_e$, $\omega_e y_e$, and $\omega_e z_e$ resulting from fittings of the vibrational spacings obtained in this VUV-PFI-PE study, the HeI experiment, and the theoretical HYP, WP, and Moss predictions are listed in Table III. The comparison in Table III shows that the vibrational constants obtained in the present VUV-PFI-PE experiment are in good accord with the theoretical predictions [2,3,5,7] and the HeI [11] photoelectron study. The uncertainties given for the Moss theoretical ω_e, $\omega_e\chi_e$, $\omega_e y_e$, and $\omega_e z_e$ values are indicative of the inadequacy of the four-parameter fit in the functional form of Eq.(5).

We have obtained the rotational constants B_{v^+} and D_{v^+} for $H_2^+(X^2\Sigma_g^+, v^+$=0-17) by fitting the rotational structures resolved in the VUV-PFI-PE vibrational bands for v^+=0-17 to the equation,

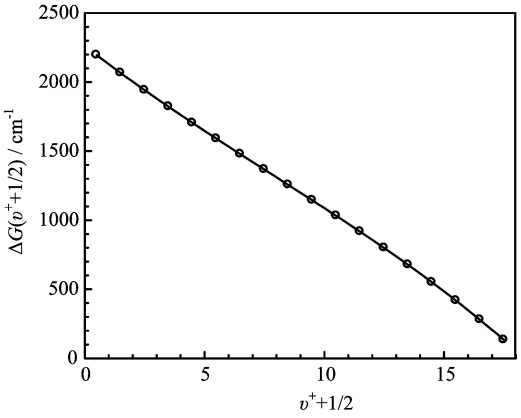

FIG. 4 Plots of the vibrational spacing of H_2^+ $\triangle G(v^+{+}1/2)$ versus $(v^+{+}1/2)$. The solid circles are values obtained based on the present VUV-PFI-PE measurement and the solid line represents the theoretical predictions of Moss (Ref.[7]).

$$\begin{aligned} v &= v_0 + B_{v^+}N^+(N^+{+}1) - D_{v^+}(N^+)^2(N^+{+}1)^2 \\ &\quad - B''_v J''(J''{+}1) + D''_v(J'')^2(J''{+}1)^2 \end{aligned} \tag{6}$$

The values of B''_v and D''_v for $H_2^+(X^1\Sigma_g^+, v''$=0) were obtained from Huber and Herzberg [13]. The resulting

DOI:10.1088/1674-0068/20/04/352-364

TABLE III Comparison of the experimental VUV-PFI-PE and HeI vibrational constants in cm^{-1} for $H_2^+(X^2\Sigma_g^+)$ with the theoretical predictions based on the HYP, WP, and Moss calculations

Vibrational constants	VUV-PFI-PE[a]	HeI[b]	HYP[c]	WP[d]	Moss[e]
ω_e	2330.79±0.33	2324.4±2.6	2326.72	2326.51	2326.5100±1.1519
$\omega_e\chi_e$	69.51±0.07	67.84±0.64	68.75	68.74	68.7405±0.2561
$\omega_e y_e$	1.135±0.006	1.000±0.059	1.089	1.089	1.08901±0.02060
$\omega_e z_e$	−0.0342±0.0002	−0.0308±0.0017	−0.0334	−0.0346	−0.03336±0.00050

[a] Experiment. This work.
[b] Experiment. Ref.[11].
[c] Theory. Ref.[2].
[d] Theory. Ref.[5].
[e] Theory. Ref.[7].

TABLE IV Comparison of rotational constants B_{v^+} and D_{v^+} in cm^{-1} for $H_2^+(X^2\Sigma_g^+, v^+=0\text{-}18)$ obtained by experimental measurements and theoretical predictions

v^+	This Work[a]		HeI[b]		Moss1[c]		Moss2[d]	
	B_{v^+}	D_{v^+}	B_{v^+}	D_{v^+}	B_{v^+}	D_{v^+}	B_{v^+}	D_{v^+}
0	29.112±0.150	0.0151±0.0058	29.6±2.5	0.03±0.08	29.14647	0.01869	29.03738	0.01679
1	27.678±0.068	0.0192±0.0042	28.1±1.1	0.04±0.04	27.60368	0.01761	27.50745	0.01608
2	26.091±0.132	0.0150±0.0054	26.4±1.1	0.03±0.03	26.10941	0.01656	26.03005	0.01541
3	24.680±0.127	0.0172±0.0052	24.8±0.5	0.02±0.02	24.67369	0.01589	24.63029	0.01517
4	23.295±0.096	0.0176±0.0040	23.6±1.1	0.03±0.04	23.28744	0.01556	23.20210	0.01420
5	21.773±0.088	0.0113±0.0036	22.3±0.4	0.03±0.01	21.90650	0.01468	21.83647	0.01367
6	20.614±0.104	0.0153±0.0041	21.0±1.3	0.02±0.04	20.57099	0.01442	20.49289	0.01317
7	19.247±0.142	0.0153±0.0057	19.0±0.3	0.00±0.01	19.23782	0.01391	19.16343	0.01273
8	17.957±0.149	0.0116±0.0057	18.3±0.5	0.04±0.03	17.91022	0.01346	17.83970	0.01234
9	16.524±0.271	0.0126±0.0109	17.2±0.6	0.05±0.03	16.56942	0.01282	16.51262	0.01200
10	15.224±0.609	0.0163±0.0053	15.0±0.8	0.00±0.04	15.22498	0.01251	15.17213	0.01174
11	13.835±0.129	0.0148±0.0052	14.5±0.5	—	13.85505	0.01227	13.80683	0.01157
12	12.488±0.179	0.0280±0.0109	12.8±0.6	—	12.45329	0.01233	12.40349	0.01153
13	11.009±0.204	0.0145±0.0082	11.1±0.5	—	10.99117	0.01247	10.94660	0.01168
14	9.558±0.040	0.0173±0.0038	9.9±1.4	—	9.44307	0.01255	9.41819	0.01214
15	7.788±0.171	0.0169±0.0069	8.3±1.1	—	7.79348	0.01315	7.79363	0.01314
16	5.947±0.049	0.0139±0.0019	—	—	5.99755	0.01440	6.00730	0.01467
17	3.9908±0.075	0.0158±0.0031	—	—	4.00263	0.01732	—	—
18	1.489±0.107	—	—	—	—	—	—	—

[a] Experiment. This work.
[b] Experiment. Ref.[11].
[c] Ref.[7]. Moss1 values are based on fitting of Moss rotational level energies for N^+=0-5.
[d] Ref.[7]. Moss 2 values are based on fitting of Moss rotational level energies for N^+=0-9.

ionic rotational constants (B_{v^+} and D_{v^+}) are compared with those reported in the HeI photoelectron study of Pollard *et al.* [11] in Table IV. Since the rotational transitions were not well-resolved in the previous HeI study, the B_{v^+} and D_{v^+} determined in the later experiment have significantly larger uncertainties than those of the present VUV-PFI-PE study. After taking into account the experimental uncertainties, the B_{v^+} and D_{v^+} values determined in the HeI are consistent with the present experimental values. We note that the rotational transitions observed here are limited to N^+=0-5, and thus, the B_{v^+} and D_{v^+} constants derived fitting the VUV-PFI-PE data are only applicable to the N^+=0-5 rotational levels. We have also obtained the B_{v^+} and D_{v^+} constants by fitting the theoretical rovibrational level energies based on the HYP, WP, and Moss calculations. Considering that the Moss calculation is the most accurate among these theoretical studies, we only list the B_{v^+} and D_{v^+} values for the Moss calculations in Table IV for comparison with the experimental values. The Moss1 and Moss2 rotational constants are obtained by fitting the Moss rotational level energies

DOI:10.1088/1674-0068/20/04/352-364

TABLE V Comparison of experimental rotational constants ($B_e{}^+$ and $\alpha_e{}^+$) in cm^{-1} and the internuclear distance (r_e) in Å for $H_2^+(X^2\Sigma_g^+)$

	VUV-PFI-PE[a]	Rydberg series[b]	HeI[c]	Moss[d]
$B_e{}^+$	29.87±0.17	30.21	29.99±0.30	29.86959
$\alpha_e{}^+$	1.4240±0.0162	1.685	1.388±0.033	1.42516
r_e	1.058±0.003	1.052	1.056±0.005	1.0579

[a] This work.
[b] Ref.[1].
[c] Ref.[11].
[d] Values derived from fitting the Moss1 B_{v^+} values. Ref.[7].

for the respective N^+=0-5 and N^+=0-9 levels. We find that the simple two-parameter function of Eq.(6) is inadequate to fit the theoretical rotational energies for a range wider than N^+=0-9. As expected, the Moss1 B_{v^+} and D_{v^+} constants are in better agreement with those of the VUV-PFI-PE experimental values. The plots of the rotational constants (B_{v^+}) for $H_2^+(X^2\Sigma_g^+$, v^+=0-17) versus v^+ obtained by the present VUV-PFI-PE measurement (solid circles) and the Moss calculation (Moss1, solid line) are shown in Fig.5. In terms of the mean variances, the experimental PFI-PE B_{v^+} and D_{v^+} values are higher than the Moss1 B_{v^+} and D_{v^+} predictions by 0.002±0.05 and 0.00151±0.00427 cm^{-1}, respectively. Since the rotational level energies for a given vibrational band were measured in a single experimental scan, the energy calibration error did not contribute to the B_{v^+} and D_{v^+} measurements. As a result, the precisions of B_{v^+} and D_{v^+} values are significantly higher than that for the vibrational spacings determined in the present VUV-PFI-PE study.

We have also determined the $B_e{}^+$ and $\alpha_e{}^+$ values for H_2^+ by fitting the experimental or theoretical B_{v^+} (v^+=0-17) values to the equation (Fig.5),

$$B_{v^+} = B_e{}^+ - \alpha_e{}^+\left(v^+ + \frac{1}{2}\right) \quad (7)$$

Based on the $B_e{}^+$ value thus determined, the internuclear distance (r_e) in Å for H_2^+ was calculated using the formula, $r_e=[h/(8\pi^2\mu B_e{}^+)]^{1/2}$, where μ is the reduced mass of H_2^+. The $B_e{}^+$, $\alpha_e{}^+$, and r_e values derived in the present VUV-PFI-PE study are given in Table V to compare with previous experimental results obtained in the HeI photoelectron study by Pollard *et al.* [11] and the Rydberg series study by Huber and Herzberg [1] and the theoretical values based on the calculation of Moss. Although the HeI and Rydberg values agree with the VUV-PFI-PE values after taking into account of the experimental uncertainties, the precisions achieved in the present PFI-PE measurement are higher than those of the HeI and Rydberg studies. As shown in Table V, the $B_e{}^+$, $\alpha_e{}^+$, and r_e values derived from the VUV-PFI-PE measurement are in excellent agreement with the values determined based on the calculation of Moss.

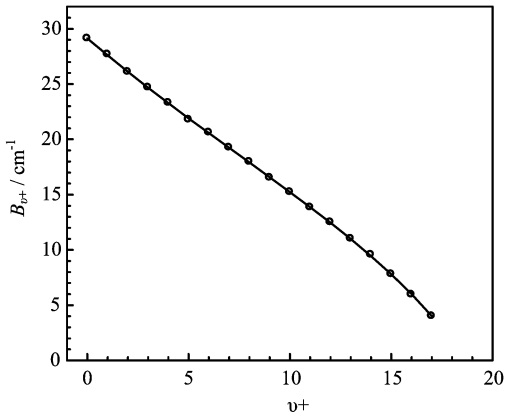

FIG. 5 Plots of the rotational constants (B_{v^+}) for $H_2^+(X^2\Sigma_g^+$, v^+=0-17) versus v^+. The solid circles are the present VUV-PFI-PE values and the solid line represents the theoretical Moss1 values (Ref.[7], see the text).

IV. CONCLUSION

We present here the rotationally resolved PFI-PE spectra for $H_2^+(X^2\Sigma_g^+$, v^+=0-18). The analysis of which has provided the rovibronic energies for v^+=0-18, the vibrational and rotational constants, and the equilibrium internuclear separation of $H_2^+(X^2\Sigma_g^+)$. As expected, these spectroscopic constants for $H_2^+(X^2\Sigma_g^+)$ are in excellent accord with high level theoretical predictions. The simulated photoelectron bands based on the BOS model are in good agreement with the VUV-PFI-PE bands of higher v^+ ($\geq$6) states, indicating strong perturbation of the relative intensities for rotational transitions occurs mainly at lower v^+ ($\leq$5) states. Thus, the rotationally resolved PFI-PE bands for $H_2^+(v^+\geq 6)$ presented here provide reliable estimates of state-to-state cross sections for direct photoionization of H_2. Furthermore, the rotationally resolved PFI-PE bands for $H_2^+(v^+\leq 5)$ represent useful data for fundamental understanding of the near resonance autoionizing mechanism using the MQDT.

DOI:10.1088/1674-0068/20/04/352-364

V. ACKNOWLEDGMENTS

This work was supported by the Director, Office of Energy Research, Office of Basic Energy Sciences, Chemical Science Division of the US. Department of Energy (No.W-7405-Eng-82) for the Ames Laboratory. C. Y. Ng also acknowledge partial supports by the DOE (No.DE-FG02-02ER15306), the AFOSR (No.FA9550-06-1-0073), and the NSF (No.CHE-0517871).

[1] A. Carrington. I. R. McNab, and C. A. Montgomeirie, J. Phys. B. At. Mol. Opt. Phys. **22**, 3551 (1989); and references therein.
[2] G. Hunter, A. W. Yau, and H. O. Pritchard, At. Data Nucl. Data Tables **14**, 11 (1974).
[3] C. L. Beckel, B. D. Hansen, and J. M. Peek, J. Chem. Phys. **53**, 3681 (1970).
[4] C. A. Leach and R. E. Moss, Annu. Rev. Phys. Chem. **46**, 55 (1995); and references therein.
[5] L. Wolniewicz and J. D. Poll, J. Chem. Phys. **73**, 6225 (1980).
[6] G. G. Balint-Kurti, R. E. Moss, I. A. Sadler, and M. Shapiro, Phys. Rev. A **41**, 4913 (1990).
[7] R. E. Moss, Mol. Phys. **78**, 371 (1993); **80**, 1541 (1993).
[8] D. M. Bishop and L. M. Cheung, J. Chem. Phys. **75**, 3155 (1981).
[9] L. Åsbrink, Chem. Phys. Lett. **7**, 549 (1970).
[10] Y. Morioka, S. Hara, and M. Nakamura, Phys. Rev. A **22**, 177 (1980).
[11] J. E. Pollard, D. J. Trevor, J. E. Reutt, Y. T. Lee, and D. A. Shirley, J. Chem. Phys. **77**, 34 (1982).
[12] F. Merkt and T. P. Softley, J. Chem. Phys. **96**, 4149 (1992).
[13] K. P. Huber and G. Herzberg, *Molecular Spectra and Molecular Structure, Vol. IV, Constants of Diatomic Molecules*, New York: Van Nostrand, (1979).
[14] F. Merkt, H. Xu, and R. N. Zare, J. Chem. Phys. **104**, 950 (1996).
[15] S. Stimson, Y. J. Chen, M. Evans, C. L. Liao, C. Y. Ng, C. W. Hsu, and P. Heimann, Chem. Phys. Lett. **289**, 507 (1998).
[16] S. Stimson, M. Evans, C. W. Hsu, and C. Y. Ng, J. Chem. Phys. **126**, 164303 (2007).
[17] C. Y. Ng, Annu. Rev. Phys. Chem. **53**, 101 (2002).
[18] P. M. Dehmer and W. A. Chupka, J. Chem. Phys. **65**, 2243 (1976).
[19] J. Berkowitz, *Photoabsorption, Photoionization, and Photoelectron Spectroscopy*, New York: Academic Press, (1979).
[20] W. H. Wing, G. A. Ruff, W. E. Lamb, and J. J. Spezeski, Phys. Rev. Lett. **36**, 1488 (1976).
[21] A. Carrington, I. R. McNab, C. A. Montgomerie, and J. M. Brown, Mol. Phys. **66**, 1279 (1989); and references therein.
[22] C. B. Richardson, K. B. Jefferts, and H. G. Dehmelt, Phys. Rev. **165**, 80 (1968).
[23] N. Y. Du and C. H. Greene, J. Chem. Phys. **85**, 5430 (1994).
[24] T. P. Softley and A. J. Hudson, J. Chem. Phys. **101**, 923 (1994).
[25] R. T. Weidman and M. G. White, *High Resolution Laser Photoionization and Photoelectron Studies*, I. Powis, T. Baer, and C. Y. Ng, Ed., *Wiley Series in Ion Chemistry and Physics*, Chichester: Wiley, 79 (1995).
[26] F. Merkt and T. P. Softley, in *High Resolution Laser Photoionization and Photoelectron Studies*, I. Powis, T. Baer, and C. Y. Ng, Ed., *Wiley Series in Ion Chemistry and Physics*, Chichester: Wiley, 119 (1995).
[27] C. Y. Ng, Int. J. Mass Spectrometry **200**, 357 (2000).
[28] C. W. Hsu, M. Evans, P. Heimann, K. T. Lu, and C. Y. Ng, J. Chem. Phys. **105**, 3950 (1996).
[29] P. Heimann, M. Koike, C. W. Hsu, M. Evans, K. T. Lu, C. Y. Ng, A. Suits, and Y. T. Lee, Rev. Sci. Instrum. **68**, 1945 (1997).
[30] M. Evans, C. Y. Ng, C. W. Hsu, and P. A. Heimann, J. Chem. Phys. **106**, 978 (1997).
[31] C. W. Hsu, M. Evans. P. A. Heimann, and C. Y. Ng, Rev. Sci. Instrum. **68**, 1694 (1997).
[32] A. D. Buckingham, B. J. Orr, and J. M. Sichel, Phil. Trans. Roy. Soc. Lond. A **268**, 147 (1970).
[33] J. Xie and R. N. Zare, J. Chem. Phys. **93**, 3033 (1990).
[34] K. Wang and V. McKoy, J. Phys. Chem. **99**, 1643 (1995).
[35] G. Herzberg, *Molecular Spectra and Molecular Structures, Vol. I, Spectra of Diatomic Molecules*, Princeton: Van Norstrand, (1950).
[36] G. K. Jarvis, Y. Song, and C. Y. Ng, Rev. Sci. Instrum. **70**, 2615 (1999).
[37] Y. Itikawa, Chem. Phys. **30**, 109 (1978); *ibid.* **28**, 461 (1978); **37**, 401 (1979).

DOI:10.1088/1674-0068/20/04/352-364